Research on An Interleaved Phase-Shift Half-Bridge LLC Resonant Converter

Shu-Po Wang[1], Min-Rui Hong[1], Ping-Tsang Wu[1], Ching-Chun Chuang [1*] and Shiue-Der Lu[2]
[1] Department of Computer Science & Information Engineering, National Formosa University, austincc@nfu.edu.tw, Taiwan
[2] Department of Electrical Engineering, National Chin-Yi University of Technology, Taiwan

Abstract-- This paper presents the analysis and simulation for a novel high-power density electric vehicle dc-dc converter. In this paper, a novel interleaved phase-shift half-bridge converter that mainly comprises two modules of a half-bridge converter and a double full-bridge rectifier is proposed. In the case of interfacing the high-voltage battery module, the isolated DC/DC converter is used to control the voltage at the input of the battery according to the battery terminal voltage and optimize the efficiency of the dc-dc converter in a wider range of operating voltage. It operates as a voltage doubler to achieve an output voltage of 450V for the charging of a high-voltage battery. The isolated dc-dc converter is operated as an LLC resonant converter owing to its advantages of simple control and soft switching operation. This converter not only has a wide range of zero-voltage-switching (ZVS) turn-on of power switches on the primary side of the transformer but also has a zero-current-switching (ZCS) turn-off of rectifier diode on the secondary side of the transformer. The proposed converter can achieve the output voltage range of 250-450V by adapting the phase shift between the two square waves. The two LLC half-bridge resonant converters are connected in parallel, and it's operated at a fixed frequency and constant duty cycle. The simplified control strategy in the proposed converter can be achieved since the switching frequency of the converter operates at the resonant point. Finally, a 3.4kW design prototype with 400V input voltage and the 250-450V output voltage is simulated to verify the effectiveness of the phase-shift mode control method.

Index Terms--Dual Full-Bridge Rectifier, Electric Vehicle, Interleaved Dual Phase-Shift Half Bridge LLC Resonant Circuit

I. INTRODUCTION

As global warming becomes severe, natural resources diminish, fuel prices rise, and economic concerns, vehicles that use electricity for energy, such as hybrid electric vehicles (HEVs), plug-in HEVs (PHEVs), battery electric vehicles (BEVs or EVs) and fuel cell electric vehicles, are gradually gaining attention. These vehicles usually require rechargeable batteries as the energy source for the electric traction system [1]. A PHEV or EV requires a higher capacity and larger size battery pack because the battery is the main energy source of the PHEV and EV. this use of electricity has increased, but the resources are limited and electricity is very precious. Among various DC-DC power converter topologies, isolated converters are the most attractive due to their simplicity and inherent characteristics such as current isolation, high power applications, soft switching, and high efficiency [2] - [3]. The development of an EV battery charger has some key requirements, an ultra-wide output voltage range [4] with galvanic isolation is required. Therefore, the design of isolated DC/DC converters needs to be adaptable and have an ultra-wide output voltage range. In recent studies, many control schemes have been proposed for isolated dc-dc converters. The simplest and most commonly used control topology for their dc-dc converters is phase shift angle control. As a popular isolated DC/DC converter, LLC resonant converter has a simple structure, power switches can through ZVS turn on and diode ZCS turn off, and in a wide load range, have high efficiency and power density [5] - [6]. In addition, conversion efficiency should be maximized by the output or battery charging process to maximize fuel savings and reduce emissions. To these requirements, higher switching frequencies and soft-switching techniques are necessary, a higher switching frequency is key to reducing the size and weight of passive components used in high-power applications. LLC resonant converters have some drawbacks. For example, if the switching frequency fs is higher than the resonant frequency f_r, the rectifier diode can't ZCS turn off and the output voltage is difficult to regulate because the voltage gain is very smooth, especially under light load conditions. Therefore, LLC resonant converters are always designed to operate in the $f_s \leq f_r$ region, where ZVS, ZCS, and output voltage regulation can be easily achieved [7]. However, achieving wide-range voltage and load regulation is still difficult while maintaining high efficiency over the entire voltage and load range when $f_s \leq f_r$ [8]. This is because once the operating frequency is far from the resonant frequency, the circulating current of the resonant tank will be increased then greatly reducing the conversion efficiency. Therefore, a trade-off between conversion efficiency and operating range is required to meet the needs of various applications.

In order to achieve a wide range of output, an interleaved phase-shifted half-bridge LLC converter has been proposed [9]. The converter control is simple, and because it is an LLC circuit, the switch can reach ZVS conduction and the rectifier diode can through ZCS turn off, reducing the switching conduction loss and rectifier diode transfer loss.

In [10] and [11], which uses a double full-bridge rectifier circuit on the secondary side. The structure can reduce voltage stress, increase the effect of energy transfer, and improve efficiency.

II. CIRCUIT OPERATION DESCRIPTION

The proposed interleaved phase-shift half-bridge LLC resonant converter is shown in Fig. 1. The proposed converter employs two LLC half-bridge resonant converters to achieve the ZVS feature. The four PWM switch S_A, S_B, S_C, and S_D are used to close or open the power circuit. The diodes D_A, D_B, D_C, D_D, D_E, and D_F are connected from nodes A and B connecting the primary power transformer to the positive and ground rails of the bridges to provide a path for the output current through the primary capacitor and load. In this converter, the upper circuit is a resonant half-bridge converter that uses two power switches S_A and S_B, transformer T_{r1} and its magnetizing inductance L_{m1}, resonant capacitor C_{r1}, and resonant inductance L_{r1}. Moreover, the lower circuit also is a resonant half-bridge converter that uses two power switches S_C and S_D, transformer T_{r2} and its magnetizing inductance L_{m2}, resonant capacitor C_{r2}, and resonant inductance L_{r2}. The primary side power switches of this converter operate with a fixed switching frequency and an approximately 50% duty cycle. By adopting the phase-shift angle of power switches S_C and S_D in the lower circuit, a wide output voltage range of 250V-450V can be achieved in the interleaved phase-shift half-bridge converter. To clarify the relationship between the output voltage V_o and phase-shift angle φ, the proposed converter will divide into two operation stages: (A) The main output voltage is 250V (V_o = 250V) and (B) The main output voltage is 450V (V_o = 450V).

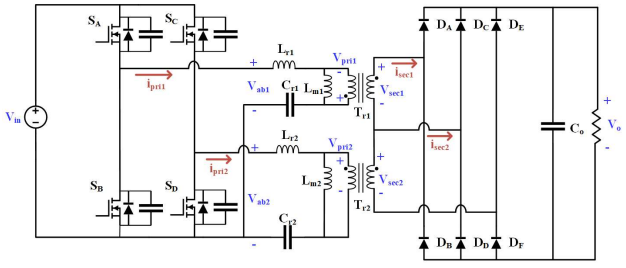

Fig. 1. The proposed interleaved LLC resonant converter.

A. The main output voltage is 250V (V_o=250V)

The mode can be divided into 5 power circuit topological states in the first half of the switching period. The key waveforms of the proposed converter with the output voltage of 250V are presented in Fig. 2. As shown in the key waveforms of the proposed converter in Fig. 2, V_{gs1}- V_{gs4} is the gate drive signal, which is used to drive the power switches S_A-S_D.V_{ab1} is the resonant tank voltage in the upper circuit, V_{ab2} is the resonant tank voltage in the lower circuit, i_{pri1} is the primary side current of the transformer T_{r1}, i_{pri2} is the primary side current of the transformer T_{r2}, i_{sec1} is the secondary side current of the transformer T_{r1}, i_{sec2} is the secondary side current of the transformer T_{r2}, and the sum of the voltage across each the secondary side of the transformer in a series is equal to V_{sec}.

Fig. 3 shows the topological stages of the proposed converter during the first switching period, and the first five modes of the proposed circuits during half of the switching cycle was shown in Fig. 2.

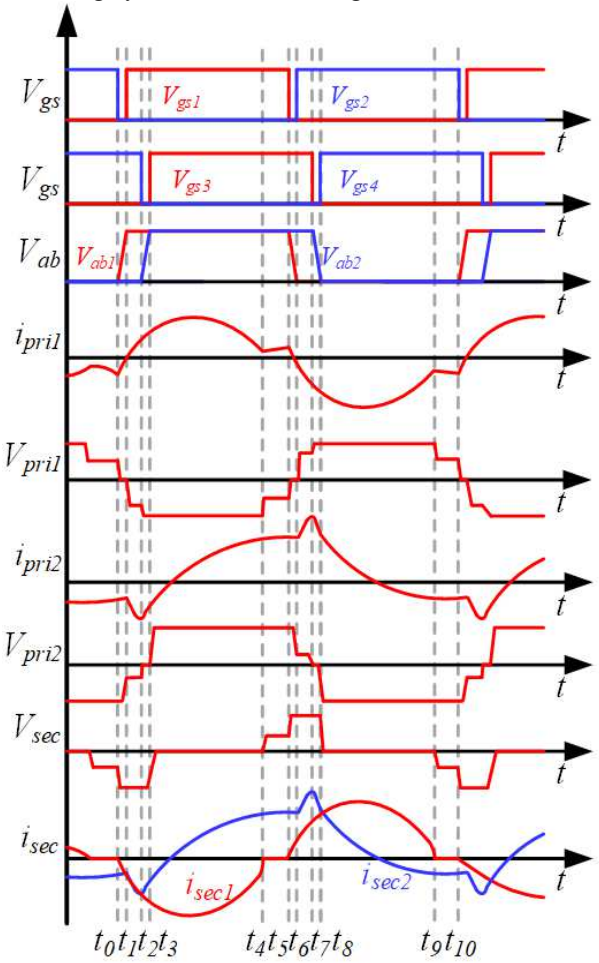

Fig. 2. The key waveforms of the proposed converter at V_o=250V.

In the second half of the switching period, the operation of the proposed converter is the same as the operation in the first half of the switching period.

Mode 1 $[t_0 - t_1]$: Mode 1 begins when the power switches S_A, S_B, and S_C are turned off, and S_D is turned on at t_0 as shown in Fig. 3(a). During this mode, the energy saved in the transformer is derived from the primary side of T_{r1} to output load and C_o is charging. After the junction capacitors of power switches S_A are discharged and the junction capacitors of switches S_B is charging, the primary current $i_{pri1} = i_{in}$ continuously flows through the antiparallel diode of power switch S_A so that the power switch S_A can be turned on with ZVS after $t = t_1$. In addition, the circulating current will continuously flow to the primary side of the transformer T_{r2}. Since the secondary side rectifier diode D_B, D_D, and D_E are turned on providing a clamping path, the voltage at the output terminal of two transformers on the secondary side is clamped to the output voltage $-V_o$.

Mode 2 $[t_1 - t_2]$: As shown in Fig. 3(b), this mode begins when S_A is turned ON. Since the junction capacitors of power switches S_A are completely discharged, the power switch S_A can achieve zero-voltage switching (ZVS). The secondary side current i_{sec1} continuous to flow through rectifiers D_B and D_E since the primary side current i_{pri1} from the negative value to the positive value. Besides, the secondary side rectifier diode D_B and D_E can be turned off

with ZCS after $t = t_1$. During this interval $t_0 - t_1$, the voltage across the primary side of the transformer T_{r1}, V_{pri1} and the transformer magnetizing voltage, V_{Lm2}, are given by

$$V_{ab1} = L_{m1}\frac{di_{pri1}(t)}{dt} + V_{cr1}(t) + L_{r1}\frac{di_{pri1}(t)}{dt} \quad (1)$$

$$nV_o = L_{m2}\frac{di_{pri2}(t)}{dt} \quad (2)$$

Mode 3 $[t_2 - t_3]$: Mode 3 begins when the power switch S_D is turn off, as shown in Fig.3(c). The primary-side current i_{pri2} of transformer T_{r2} continuous to flow through the leakage inductor L_{r2}. The current i_{pri2} begins discharging the junction capacitors of power switch S_C and charging the junction capacitor of power switches S_D so that the power switch S_C can be turned on with ZVS after $t = t_2$. Since the voltage across the primary of the transformer T_{r1} is V_{in} and the voltage across the primary of the transformer T_{r2} is opened. As a result, the secondary winding of T_{r2} are shorted so that rectifier D_C is conduct. The secondary winding of T_{r1} is delivered the powers from the input to output through D_B and D_C, and C_C is charging. This enables the secondary rectifier output voltage V_{sec1} to be clamped to $-V_o$. The V_{ab2} and V_{Lm1} can be expressed as follows:

$$V_{ab2} = -L_{m2}\frac{di_{pri2}(t)}{dt} + V_{cr2}(t) - L_{r2}\frac{di_{pri2}(t)}{dt} \quad (3)$$

$$nV_o = L_{m1}\frac{di_{pri1}(t)}{dt} \quad (4)$$

Mode 4 $[t_3 - t_4]$: This mode begins when the power switch S_C is turned ON, as shown in Fig.3 (d). The voltage V_{Sc} across the junction capacitor of power switch S_C to be clamped to 0. As a result, the power switch S_C can be turned with ZVS after $t = t_2$. Meanwhile, the primary-side current i_{pri2} of transformer T_{r2} continuous to flow through power switch S_A and S_C from the negative value to the positive value. Since the voltages across the primary of the transformer T_{r1} and T_{r2} are V_{in}. As a result, during the topological mode when the secondary side rectifier diode D_B and D_C are continuous conducting, shown in Fig. 3(d), secondary current i_{sec1} continuous charging output capacitance and output load. Meanwhile, the secondary side rectifier diode D_E is turned off with ZCS after $t = t_3$, and D_F is conducted. This enables the secondary rectifier output voltage V_{sec2} to be clamped to $-V_o$. The primary-side voltage V_{ab1} of transformer T_{r1} and the primary-side voltage V_{ab2} of transformer T_{r2} can be expressed as follows:

$$V_{ab1} = -L_{m1}\frac{di_{pri1}(t)}{dt} + V_{cr1}(t) - L_{r1}\frac{di_{pri1}(t)}{dt} \quad (5)$$

$$V_{ab2} = -L_{m2}\frac{di_{pri2}(t)}{dt} + V_{cr2}(t) - L_{r2}\frac{di_{pri2}(t)}{dt} \quad (6)$$

Mode 5 $[t_4 - t_5]$: This mode begins when D_B is turned ON. Since the secondary side rectifier diode D_B is turned off with ZCS, the secondary side voltage V_{sec1} of transformer T_{r1} is equal to zero so that the primary side energy cannot transfer to output load through the transformer T_{r1}. Moreover, the secondary side diodes D_C and D_F are continuous conduct so that the voltage of the transformer on the secondary side V_{sec2} is clamped to $-V_o$.

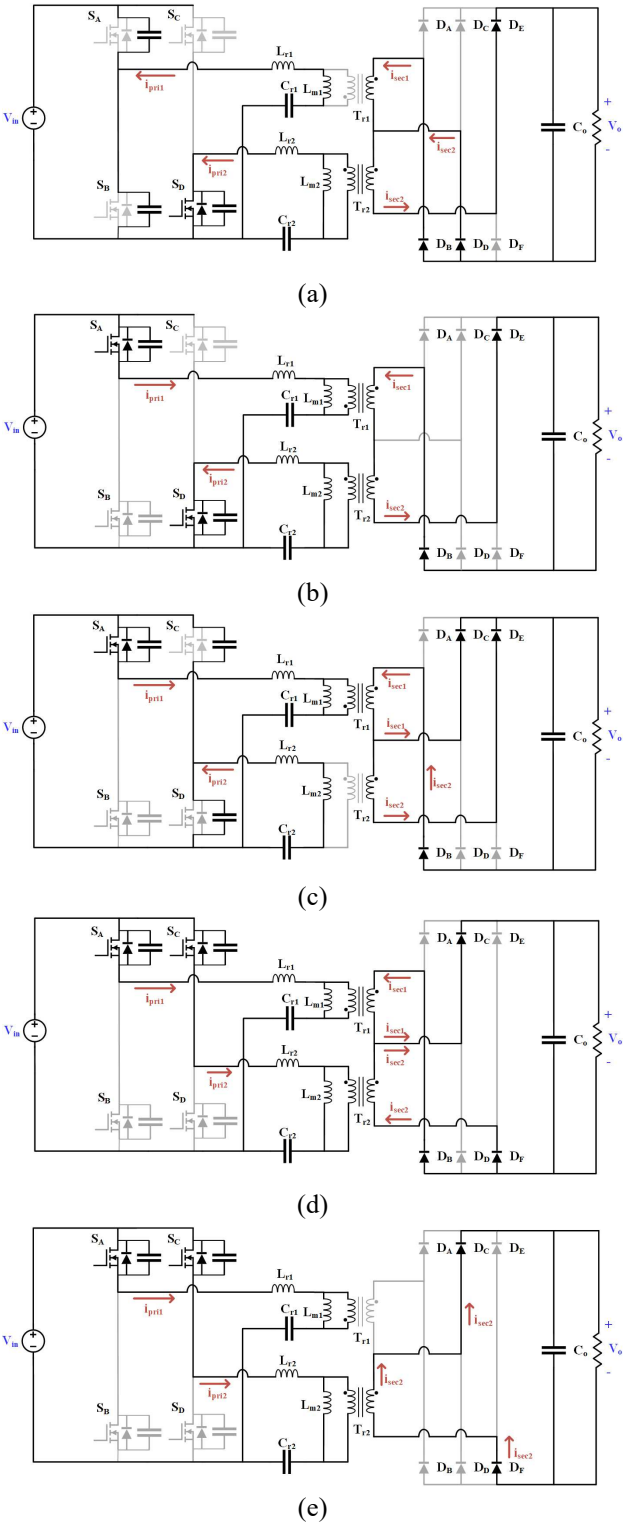

Fig. 3. Equivalent circuits of half switching period at V_o=250V.

B. The main output voltage is 450V (V_o=450V)

This mode can be divided into 4 power circuit topology states in each half-switching period. The key waveforms are presented in Fig. 3. Fig. 4 shows the equivalent circuits of the first four modes over a half-switching cycle and the next four modes are symmetrical. In this mode, i_{sec1} is the same as i_{sec2}. Since the circuit characteristic, the secondary side rectifier diodes D_D isn't conducted.

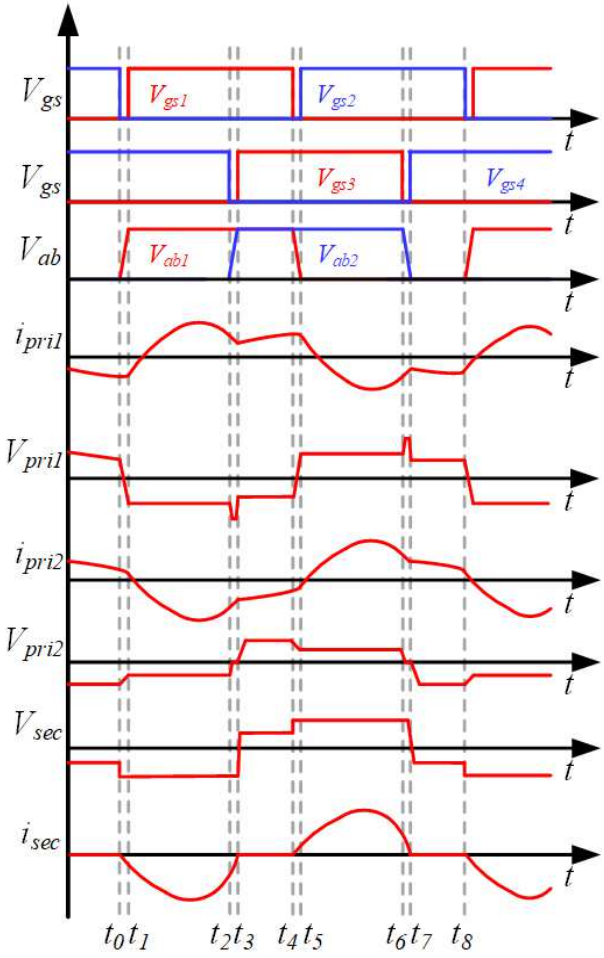

Fig. 4. The key waveforms of the proposed converter at V_o=450V.

Mode 1 $[t_0 - t_1]$: Mode 1 begins when the power switches S_A, S_B, and S_C are turned off, and S_D is turned on at t_0 as shown in Fig. 5(a). During this mode, the energy saved in the transformer is derived from the primary side of T_{r2} to output load and C_o is charging. After the junction capacitors of power switches S_A are discharged and the junction capacitors of switches S_B is charging, the primary current $i_{pri1} = i_{in}$ continuously flows through the antiparallel diode of power switch S_A so that the power switch S_A can be turned on with ZVS after $t = t_1$. In addition, the circulating current will continuously flow to the primary side of the transformer T_{r2}. Since the secondary side rectifier diode D_B and D_E are turned on providing a clamping path, the voltage at the output terminal of two transformers on the secondary side is clamped to the output voltage $-V_o$. Meanwhile, the secondary side current i_{sec1} and i_{sec2} are started to increase in the negative direction.

Mode 2 $[t_1 - t_2]$: This mode begins when the power switch S_A is turned ON, as shown in Fig.3 (b). At t_1, since the parasitic capacitance S_{AC1} of S_A has been discharged, S_A is turned on through ZVS. Meanwhile, the inductor current i_{pri1} changes from negative to positive. The secondary side rectifier diodes D_C is conducting, D_B and D_E are conduct

$$V_{ab1} = L_{m1}\frac{di_{pri1}(t)}{dt} + V_{cr1}(t) + L_{r1}\frac{di_{pri1}(t)}{dt} \quad (7)$$

$$nV_o = L_{m1}\frac{di_{pri1}(t)}{dt} - L_{m2}\frac{di_{pri2}(t)}{dt} \quad (8)$$

Mode 3 $[t_2 - t_3]$: This mode begins when the power switch S_D is turned OFF, as shown in Fig.3 (d). The inductor current i_{pri2} is negative at this time, the parasitic capacitance of S_C is discharged, the parasitic capacitance of S_D is charging, and the inductor current i_{pri2} can make S_C achieve ZVS turn on, the rectifier diodes D_C is turned off with zero current, and D_B and D_E continue to conduct.

$$V_{ab1} = L_{m1}\frac{di_{pri1}(t)}{dt} + V_{cr1}(t) - L_{r1}\frac{di_{pri1}(t)}{dt} \quad (9)$$

$$V_{ab2} = -L_{m2}\frac{di_{pri2}(t)}{dt} + V_{cr2}(t) - L_{r2}\frac{di_{pri2}(t)}{dt} \quad (10)$$

$$nV_o = L_{m1}\frac{di_{pri1}(t)}{dt} \quad (11)$$

Mode 4 $[t_3 - t_4]$: This mode begins when the power switch S_C is turned ON, as shown in Fig.3 (d). At t_3, since the parasitic capacitance of S_C has been discharged, S_C is turned on through ZVS. Meanwhile, the inductor current i_{pri2} slowly turns from negative to positive. The secondary side rectifier diodes D_B and D_E are turned off with zero current.

$$V_{ab1} = L_{m1}\frac{di_{pri1}(t)}{dt} + V_{cr1}(t) + L_{r1}\frac{di_{pri1}(t)}{dt} \quad (12)$$

$$V_{ab2} = -L_{m2}\frac{di_{pri2}(t)}{dt} + V_{cr2}(t) - L_{r2}\frac{di_{pri2}(t)}{dt} \quad (13)$$

$$nV_o = L_{m1}\frac{di_{pri1}(t)}{dt} - L_{m2}\frac{di_{pri2}(t)}{dt} \quad (14)$$

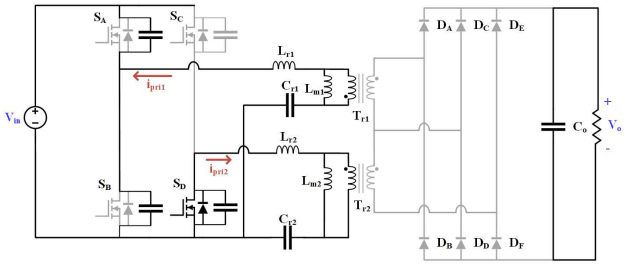

(a)

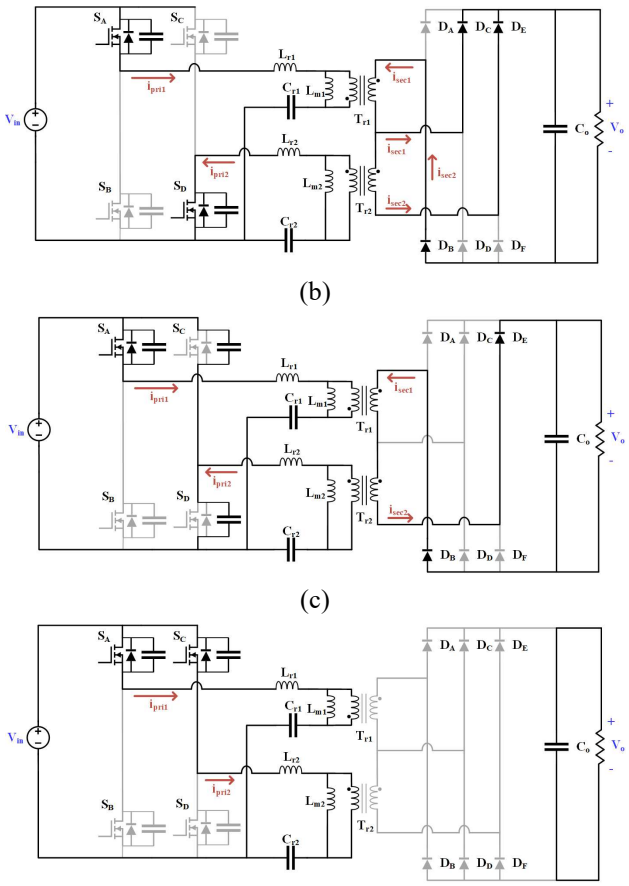

Fig. 5. Equivalent circuits of half switching period at V_o=450V.

C. Circuit Simulation Result

In order to verify the feasibility of the interleaved phase-shifted half-bridge LLC resonant conversion circuit proposed in this study, POWERSIM is used for simulation analysis in this study. The simulation results are shown in Fig. 7 and 8. From top to bottom are the power switches Q_A, Q_B, Q_C, and Q_D, V_{ab} is the upper resonant tank voltage, V_{ab2} is the lower tank voltage, and the transformer primary side input current i_{pri1}, the lower side of the transformer primary side input current i_{pri2} and output voltage V_o. Simulating the proposed phase-shift modulated interleaved LLC converter of 1kW, and adopting the phase-shift to achieve the ideal output voltage. Through simulating waveforms with different phase shift angles, it can be known that increasing the phase shift angle can increase the output voltage, and decreasing the phase shift angle can reduce the output voltage.

TABLE I
DESIGN PARAMETERS OF THE PROTOTYPE

Components	Values
V_{in}(Input voltage)	400V
V_o(Output voltage)	250-450V
$L_{r1,2}$(Resonant inductor)	25uH
$C_{r1,2}$(Resonant capacitor)	100nF
$L_{m1,2}$(Magnetizing inductor)	312uH
C_o(Output capacitor)	235uF
$n_{1,2}$(Turns ratio)	10:12
f_s(Switching frequency)	100kHZ

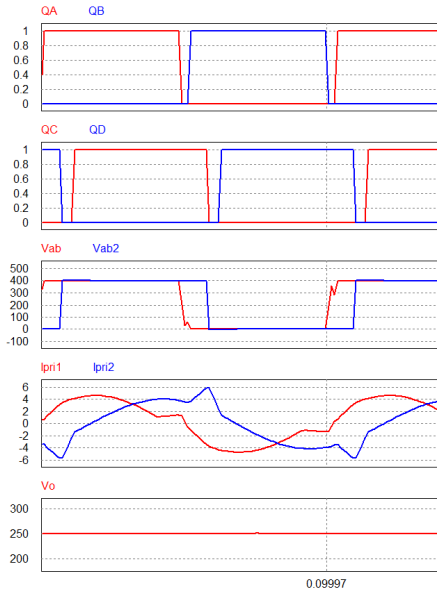

(a)

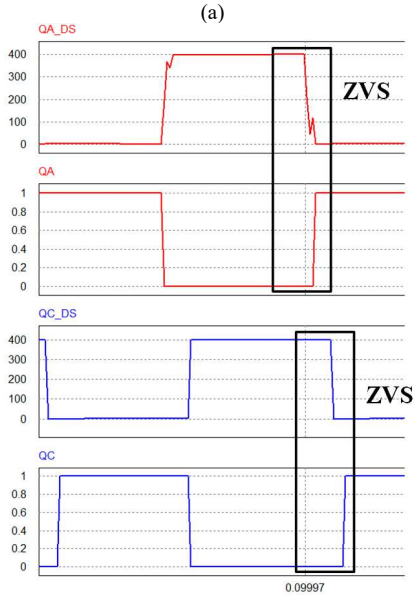

(b)

Fig. 7. The simulation waveforms at P_o=1kW, V_o=250V.

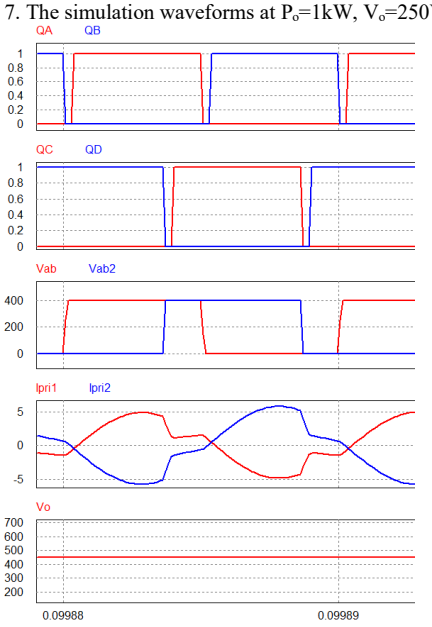

(a)

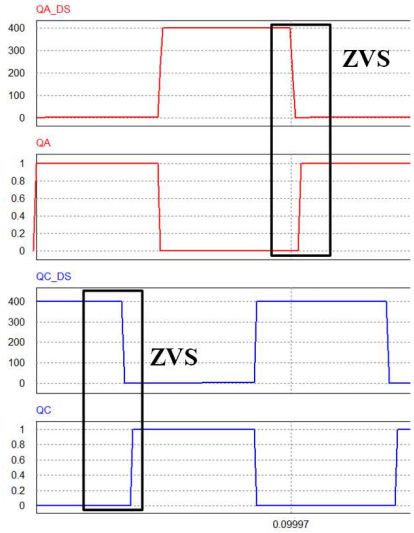

(b)

Fig. 8. The simulation waveforms at P_o=1kW, V_o=450V.

III. Circuit Analysis

A. Voltage Stress of Secondary Rectifier

At V_o=250V, on the secondary side, there are two energy transfer modes. In the mode shown in Fig. 9(a), the second side voltage V_{sec1} is equal to 0.25V_o, and the second side voltage V_{sec2} is equal to 0.75V_o. In this mode, since the rectifier diodes D_B and D_E are conducted, the V_{sec} voltage is clamped at V_o, so the voltage stress of D_C and D_E can be obtained as

$$V_{DC} = V_o - 0.75V_o \quad (15)$$

$$V_{DD} = V_o - 0.25V_o \quad (16)$$

In another mode shown in Fig. 9(b), since the rectifier diodes D_C and D_F are conducted, V_{sec} is clamped at V_o, and the D_A and D_B voltage stresses can be obtained as

$$V_{DA} = 0.6V_o \quad (17)$$

$$V_{DB} = V_o - 0.6V_o \quad (18)$$

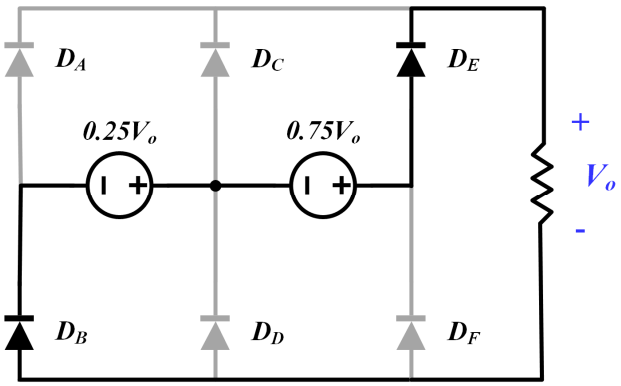

(a)

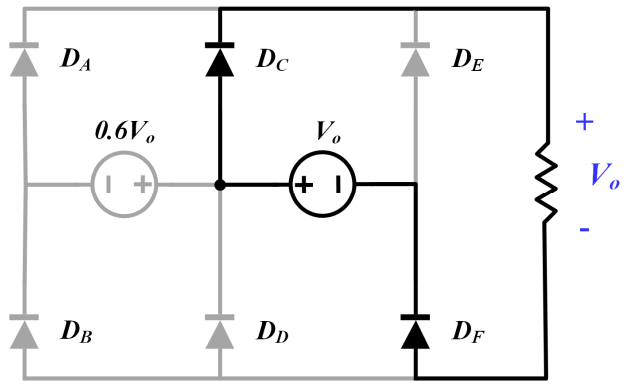

(b)

Fig. 9. Equivalent circuit of rectifier stage in the case that V_o=250V. (a) both LLC HB converters transfer the power (b) only one LLC HB converter transfers the power.

At V_o=450V, on the secondary side, there are also two energy transfer modes. In the mode shown in Fig. 10(a), the second side voltage V_{sec1} and V_{sec2} are equal to 0.5V_o. In this mode, since the rectifier diodes D_B, D_C, and D_E are conducted, the V_{sec} voltage is clamped at V_o, so the voltage stress of D_D can be obtained as

$$V_{DD} = 0.5V_o \quad (19)$$

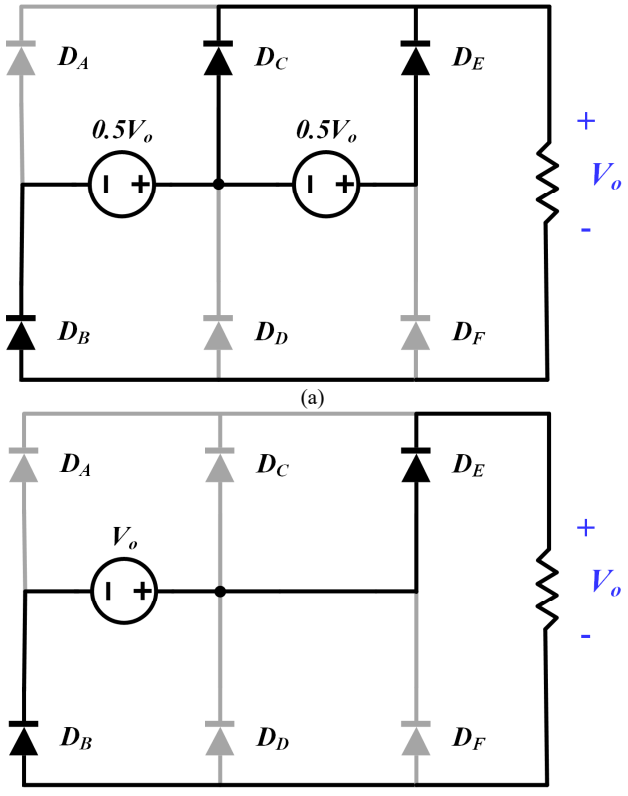

Fig. 10. Equivalent circuit of rectifier stage in the case that V_o=450V. (a) both LLC HB converters transfer the power (b) only one LLC HB converter transfers the power.

In another mode shown in Fig. 9(b), since the second side voltage V_{sec2}=0V is equivalent to a short circuit, the rectifier diodes D_B and D_E are conducted, V_{sec} is clamped at V_o, and the D_A, D_C, and D_F voltage stresses can be obtained as

$$V_{DA,\,DC,\,DF} = V_o \tag{20}$$

$$V_{DD} = 0V \tag{21}$$

B. Transformer Utilization

The proposed research on the interleaved phase-shifted half-bridge LLC resonant conversion circuit will have more application value to analyze the utilization rate of magnetizing components because the two input voltages on the primary side of the transformer are connected in reverse series and the two output voltages on the secondary side are connected in series. Considering the literature [12], if the CC-CV charging method is used in the battery high voltage range of 250~450V, if the output current I_o is the current $I_{Battery}$ flowing into the high voltage battery module (I_o=$I_{Battery}$), the transformer utilization of the converter (T.U) can be expressed as

$$T.U. = \frac{P_{o,\max}}{P_{PSHBLLC1,\max} + P_{PSHBLLC2,\max}} = \frac{V_{o\_\max} * I_o}{V_{o\_\max} * I_o + V_{o\_\min} * I_o} = \frac{450V * I_o}{450V * I_o + 250V * I_o} = 0.64 \tag{22}$$

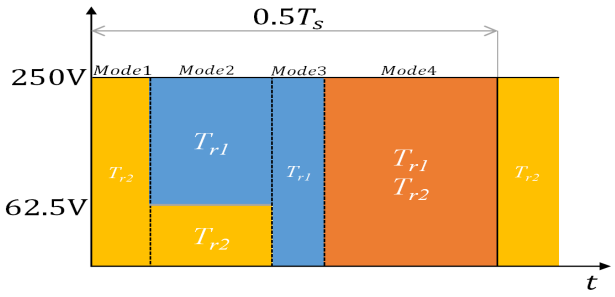

Fig. 11. Transformer utilization at V_o=250V

The low transformer utilization means that the total size or effective area of the transformer used is very large compared to a single transformer in a conventional phase-shifted full-bridge converter with the same power capability developed for an on-board charger.

At V_o=250V, in energy transmission mode 1, V_{sec2}=$V_{o(min)}$ and V_{sec1}=0, the upper side transformer is regarded as short circuits, so only the lower side transformer transmits energy, so there will be no problem with transformer utilization.

In energy transmission mode 2, the upper side voltage and the lower side voltage of the secondary side are V_{sec1}=250V*0.75 and V_{sec2}=250V*0.25, respectively. Transformer utilization (T.U) can be expressed as

$$T.U. = \frac{(V_{o\_\min}) * I_o}{(V_{o\_\min} * 0.75) * I_o + (V_{o\_\min} * 0.25) * I_o} = \frac{250V * I_o}{187.5V * I_o + 62.5V * I_o} = 1 \tag{23}$$

In energy transmission mode 3, V_{sec1}=$V_{o(min)}$ and V_{sec2}=0 are regarded as short circuits, so only the upper side transformer transmits energy, so there will be no problem with transformer utilization.

In energy transmission mode 4, V_{sec1}=250V and V_{sec2}=250, T_{r1} and T_{r2} connected in parallel transmit energy.

At V_o=450V, in energy transmission mode 1, the upper side voltage and the lower side voltage of the secondary side are V_{sec1}=450V/0.5 and V_{sec2}=450V/0.5, respectively. Transformer utilization (T.U) can be expressed as

$$T.U. = \frac{(V_{o\_\max}) * I_o}{(V_{o\_\max} * 0.5) * I_o + (V_{o\_\max} * 0.5) * I_o} = \frac{450V * I_o}{225V * I_o + 225V * I_o} = 1 \tag{24}$$

In energy transmission mode 2, V_{sec1}=$V_{o(max)}$ and V_{sec2}=0 are regarded as short circuits, so only the upper side transformer transmits energy, so there will be no problem with transformer utilization.

In energy transmission mode 3, because the switches S_A and S_C are closed, there is no energy transmission, and the energy can only flow back on the primary side, so the rectifier diodes on the secondary side are all closed, and the load is supplied by the output capacitor C_o.

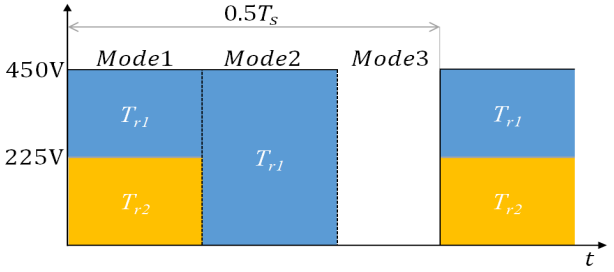

Fig. 12. Transformer utilization at V_o=450V

IV. Conclusions

The application of DC-DC isolated power converters with wide output and high power density performance in high-voltage battery charging systems is an important research topic. The interleaved phase-shifted half-bridge LLC resonant converter proposed in this study uses a two-transformer architecture. Interleaved half-bridge resonant LLC converters are used on the primary side of the transformer and dual full-bridge rectifiers are used on the secondary side of the transformer. The proposed converter's control method is simple, all four power switches can through ZVS turn on to reduce the loss because the LLC resonant circuit topology is used, and the simulation results are shown in Fig. 7 and 8. From the simulation results, it can be known that through phase shift to adapt the output voltage under different load operations is feasible. Finally, the efficiency line graph is shown in Fig. 13 and 14. There shows the efficiency on output voltage 250V and 450V, respectively. Under different rectification structures, using dual full bridge rectification structure efficiency is higher than one full bridge structure, the maximum efficiency reaches 97%, and there is room for improvement.

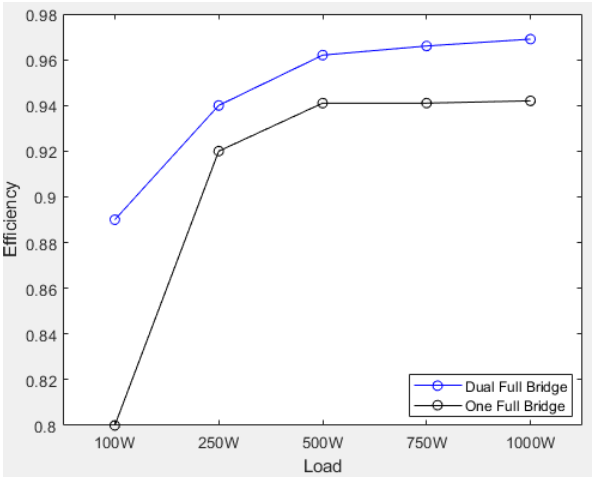

Fig. 13. Efficiency with different rectifier circuits at 250V

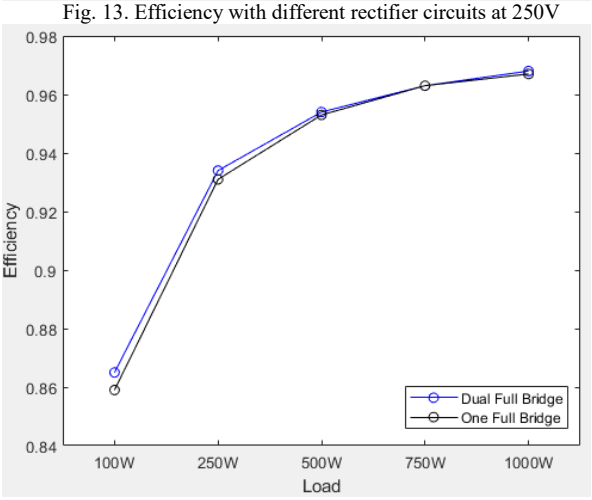

Fig. 14. Efficiency with different rectifier circuits at 450V

ACKNOWLEDGMENT

The authors would like to acknowledge the financial support of the National Science and Technology Council of Taiwan through no.109-2221-E-150-041-MY3

REFERENCES

[1] I. Aharon and A. Kuperman, "Topological overview of powertrains for battery-powered vehicles with range extenders," IEEE Trans. PowerElectron., vol. 26, no. 3, pp. 868–876, Mar. 2011.

[2] X. Fang, H. Hu, Z. J. Shen and I. Batarseh, "Operation Mode Analysis and Peak Gain Approximation of the LLC Resonant Converter," in IEEE Transactions on Power Electronics, vol. 27, no. 4, pp. 1985-1995, April 2012.

[3] H. Hu, X. Fang, F. Chen, Z. J. Shen and I. Batarseh, "A Modified High-Efficiency LLC Converter With Two Transformers for Wide Input-Voltage Range Applications," in IEEE Transactions on Power Electronics, vol. 28, no. 4, pp. 1946-1960, April 2013.

[4] M. I. Shahzad, S. Iqbal, and S. Taib, "A wide output range HB-2LLC resonant converter with hybrid rectifier for PEV battery charging," IEEE Trans. Transp. Electrific., vol. 3, no. 2, pp. 520–531, Jun. 2017.

[5] G. Li, J. Xia, K. Wang, Y. Deng, X. He, and Y. Wang, "Hybrid modulation of parallel-series LLC resonant converter and phase-shift full-bridge converter for a dual-output DC-DC converter," IEEE J. Emerg. Sel. Topics Power Electron., vol. 7, no. 2, pp. 833–842, Jun. 2019.

[6] X. Fang, H. Hu, Z. J. Shen, and I. Batarseh, "Operation mode analysis and peak gain approximation of the LLC resonant converter," IEEE Trans. Power Electron., vol. 27, no. 4, pp. 1985–1995, Apr. 2012.

[7] Z. Hu, L. Wang, H. Wang, Y.-F. Liu, and P. C. Sen, "An accurate design algorithm for LLC resonant converters-part I," IEEE Trans. Power Electron., vol. 31, no. 8, pp. 5435–5447, Aug. 2016.

[8] F.Musavi, M. Craciun, D. S. Gautam,W. Eberle, and W. G. Dunford, "An LLC resonant DC-DC converter for wide output voltage range battery charging applications," IEEE Trans. Power Electron., vol. 28, no. 12, pp. 5437–5445, Dec. 2013.

[9] B. Xue, H. Wang, J. Liang, Q. Cao and Z. Li, "Phase-Shift Modulated Interleaved LLC Converter With Ultrawide Output Voltage Range," in *IEEE Transactions on Power Electronics*, vol. 36, no. 1, pp. 493-503, Jan. 2021.

[10] I. -O. Lee and G. -W. Moon, "Half-Bridge Integrated ZVS Full-Bridge Converter With Reduced Conduction Loss for Electric Vehicle Battery Chargers," in *IEEE Transactions on Industrial Electronics*, vol. 61, no. 8, pp. 3978-3988, Aug. 2014.

[11] Y. Zhou, G. Chen, F. Wang, J. Zeng and L. Huang, "A ZVZCS Hybrid Dual Full-Bridge Converter Suitable for Wide Input Voltage Range," in *IEEE Transactions on Industrial Electronics*, vol. 68, no. 12, pp. 12058-12068, Dec. 2021.

[12] I. Lee, and G. Moon, "Half-bridge integrated ZVS full-bridge converter with reduced conduction loss for electric vehicle battery chargers," *IEEE Trans. Ind. Electron.*, vol. 61, no. 8, pp. 3978–3988, Aug. 2014.